ΠΑΝΕΠΙΣΤΗΜΙΟ ΚΡΗΤΗΣ
UNIVERSITY OF CRETE

Nik|hef

UNIVERSITY OF CRETE

DEPARTMENT OF PHYSICS

Strangeness azimuthal angular correlations in pp collisions using PYTHIA at $\sqrt{s} = 14 TeV$

THESIS BSc PHYSICS

Author:
Nefeli Bogdanou

Under the supervision of:
Dr. Panos Christakoglou
Dr. Vasilis Niarchos
Dr. Achilleas Porfyriadis
PhD Candidate Rik Spijkers

June 2024

Abstract

This study seeks to contribute to our understanding of hadronization processes within the domain of QCD, a theory crucial for describing subatomic interactions. Hadronization, the process by which quarks and gluons are confined into bound states of particles known as hadrons, remains a challenge within QCD. The purpose of this study is to investigate this mechanism by analyzing the azimuthal angular correlations of hadrons containing strange and/or anti-strange quarks. Specifically, we examine the azimuthal angular correlations of charged K mesons and $(\overline{\Lambda})$, Ξ^+- and Ω^+- baryons across various p_{T} ranges of the trigger and associate particles. Through this examination, we aim to decode the patterns and interactions governing hadronization processes, contributing to our knowledge of QCD.

Contents

1 Introduction

Scientific discoveries have continually revealed deeper layers of the natural world and the more we "zoom in", the more we discover. Our knowledge in scientific fields, especially in physics, has developed to a great extent. Over time, we came to understand the laws that govern the classical world and we delved into the microcosm, uncovering the complexities of quantum mechanics, which marked the beginning of a new era, revolutionizing our knowledge of particle physics. We now know that matter is composed of fundamental particles, such as quarks, leptons and bosons (including gluons, the carriers of the strong force), which interact through the four fundamental forces: the strong and weak nuclear forces, the electromagnetic force and gravity. The Standard model explains the fundamental particles and their interactions, as shown in Figure 1, covering three of the four basic forces in nature: electromagnetism, the weak nuclear force, and the strong nuclear force. Gravity, however, is not included. A more complete theory that is able to explain all four forces sufficiently remains an open issue.
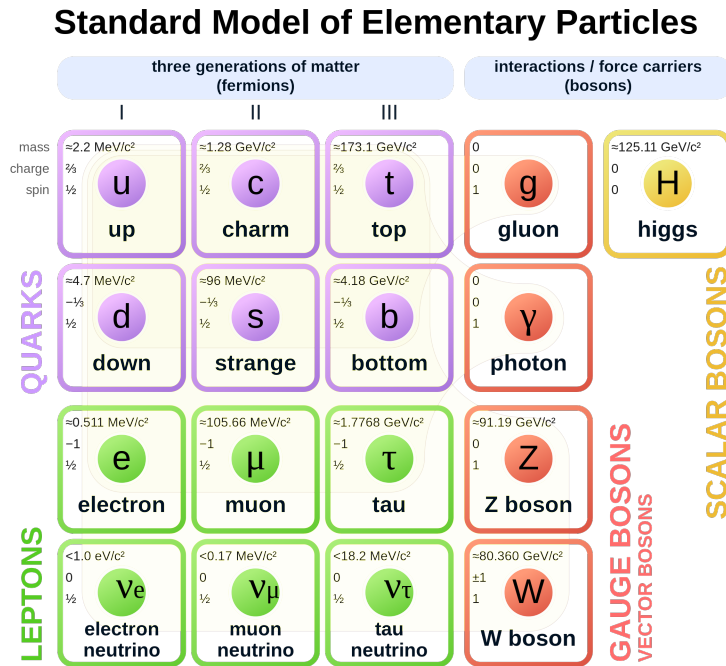

Figure 1: The Standard Model. Figure taken from [1]

This study will primarily focus on physics within the context of the strong interaction, as described by quantum chromodynamics (QCD), providing insight into how matter is formed, the synthesis of elements etc. QCD is a theory that explains how quarks and gluons interact and bind together to form protons, neutrons, and other hadrons, a mechanism guided by the strong nuclear form. The strong force, in particular, can be studied through strange quarks in hadronic matter, as it is done in this project. Understanding strangeness, a quantum number strange quarks possess, is important to understand fundamental forces and interactions of the strong force.

In QCD, quarks carry a property called "color charge," which comes in three types -red, blue and green- and their anticolors. Gluons are the force carriers that mediate the interactions between quarks by exchanging color charge [2]. In nature quarks are never found in isolation but are confined within hadrons, such as protons and neutrons, which are color-neutral combinations of quarks. The strong force binds quarks together, becoming stronger as they are pulled apart, a phenomenon known as confinement [2]. This process is evident during high-energy collisions, where quarks and gluons are initially produced in a free state and immediately undergo hadronization. During this transition, "strings" of gluons form and break, creating new quark-antiquark pairs, which ultimately result in the observable particles detected in experiments.

The coupling constant [2] in QCD, often denoted as α_s, is an equally important characteristic of the strong interaction that measures the strength of the interaction between quarks and gluons. The QCD coupling constant is not fixed, it varies with the distance between quarks or, equivalently, the energy scale of the interaction. The concept of asymptotic freedom is essential for understanding the relationship between confinement and the coupling constant. At very short distances (high energies), the QCD coupling constant α_s becomes small, indicating that quarks interact weakly and can move almost freely. However, at larger distances (low energies), the coupling constant increases significantly, leading to a strong interaction that is believed to be related to the confinement of quarks within hadrons. This dependance of the coupling constant on the energy scale is a fundamental feature of QCD, exhibiting asymptotic freedom at high energies, while indicating an association to the confinement of quarks at low energies.

2 Theoretical Background

2.1 From theory to experiments - Modern day physics

Quantum Chromodynamics (QCD) is the field theory that describes how the quarks and gluons, some of the fundamental constituents of ordinary matter, interact via the the strong force. There are some mechanisms, nonetheless, whose processes are not known or able to be described in detail. Researchers are making an effort to give insight and answer modern day physics questions. One of these processes is hadronization and the aim of this study is to contribute in our understanding of this mechanism. Essentially, this research, despite being partially guided by QCD theory, it is performed within an experimental context. Experimental data precede theory at the moment posing a challenge in modern particle physics, which is to reconcile the theory with the results/data acquired so far.

2.1.1 Hadronization

Hadronization is the process by which quarks and gluons combine in colourless hadrons after high-energy collisions. It is essential to study the mechanism behind hadronization, as it allows us to understand the fundamental forces and the ordinary matter better, as well as the behaviour of matter in high energy phenomena. It is a direct consequence of QCD dynamics and the confinement principle, illustrating how these fundamental concepts govern the behavior of matter at the smallest scales. The process of hadronization [2] can be probed with high-energy collisions, like those occurring in particle accelerators, that involve quarks and gluons. These particles then undergo parton showering, generating a cascade of quarks and gluons, known as partons. Due to color confinement dictated by QCD, partons tend to confine into color-neutral combinations. As the quarks move apart at high velocities, the energy stored in the color field increases, leading to the creation of new quark-antiquark pairs through mechanisms such as string fragmentation. According to the Lund String Model, which is explained in more detail in the following section, the colour field becomes compressed into a narrow tube, and as quarks separate further, more energy is gained, allowing the string to "cut" into smaller pieces, only by forming additional quark-antiquark pairs. These pairs ultimately combine to form colorless hadrons. Typically, this process ends with two jets of hadrons, aligning with the initial quark and antiquark directions, a common observation in high-energy experiments.

Experiments performed in accelerators such as, the LHC and the RHIC, have provided valuable insight into hadronization. For instance, experiments like ATLAS [3] and CMS [4] have studied jet formation and properties in proton-proton and heavy-ion collisions at high energies, providing data used in testing theoretical models of hadronization and understanding the behavior of quark-gluon plasma. Similarly, the STAR [5] and PHENIX [6] collaborations -RHIC-, have investigated hadronization processes in collisions involving heavy nuclei, such as gold and copper, contributing to our understanding of the phase diagram of nuclear matter and the transition from quark-gluon plasma to hadronic matter. Despite these efforts though, hadronisation remains a complex phenomenon, which is not yet completely understood. No theory can describe it comprehensively, indicating the need to use different phenomenological models to describe the experimental data. Although, these models are based on QCD, they cannot be regarded as first-principles theoretical descriptions.

2.1.2 Strangeness enhancement

At high tempreratures and energy densities nuclear matter transitions to the Quark Gluon Plasma (QGP), which is a state when quarks and gluons are not confined inside the typical hadronic bags. This results in a higher production of strange hadrons. Strangeness enhancement, which is this higher production of strange baryons, was reported in high multiplicity proton-proton (pp) collisions as well [7], which are the type of collisions used in the simulations performed in this study. According to the ALICE collaboration [7], the intergrated yields of strange particles and strange hadrons (mesons and baryons) relative to pions noticed an increase with the event charged-particle multiplicity. It is important to mention that this phenomenon -strangeness enhancement- on a microscopic level is not yet understood.

Figure 2 [7] following the above statement regarding strange production in proton-proton collisions, illustrates the intergrated yield ratios of various particles to pions as a function of multiplicity, measured within the pseudorapidity $|\eta| < 0.5$. The particles analysed include K, Λ, Ξ and Ω particles, all of which contain strange quarks. The experimental data are compared to predictions from various models, including PYTHIA, a program used in the analysis of this study, which is described in the subsequent section. We notice that the yield rations increase with increasing strangeness and also with increasing multiplicity. An important observation from this plot is that PYTHIA does not accurately predict the production of strange hadrons particularly as strangeness increases.
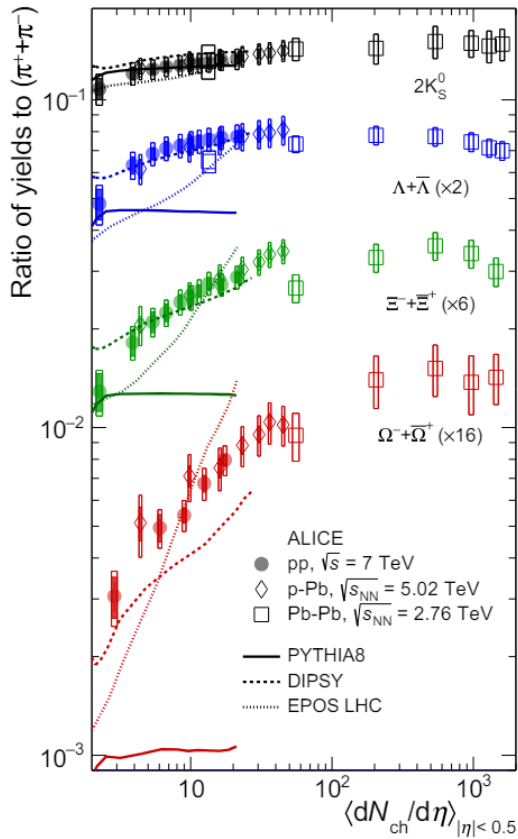

Figure 2: Figure taken from [7]

2.2 PYTHIA

PYTHIA [8], which was used for the analysis of this project, is a Monte Carlo event generator program utilized for simulating particle collisions at high energies. To further explain the above statement, in particle physics, event is the result of a collision or decay and an event generator is a numerical algorithm that generates random sequences of simulated events, based on known or hypothetical laws of nature. It is designed to describe collisions between elementary particles such as electrons (e^+), positrons (e^-), protons (p), and their antiparticles in various combinations, including heavy-ion collisions. The program is mainly coded in C++ and it allows users to specify input parameters using configuration files, which contain various settings and options that control the behaviour of the simulations or with modifying the source code of PYTHIA directly. Moreover, the program encompasses a comprehensive set of theoretical models covering multiple physics aspects, including total and partial cross sections, hard and soft interactions, parton distributions, initial and final state parton showers, matching and merging of matrix elements and showers, multiparton interactions, hadronization/fragmentation, and decay processes. Additionally, it features interfaces for data input and output with other software.

Given the complexity of hadron collisions and the lack of a comprehensive theory to predict event properties over this full range, PYTHIA provides a valuable tool for studying these processes. Hadron collisions involve the production of various particles and phenomena, and to address this complexity, phenomena are divided into a number of components based on time or energy (or transverse momentum) ordering. One crucial aspect of hadron collisions is hadronization (fragmentation) [8]. In PYTHIA this mechanism operates through the Lund string model, adapting to recent advancements in fragmentation dynamics, allowing researchers to investigate the production and the properties of hadrons in these collisions.

The Lund String Model [9], a phenomenological hadronization model, is rooted in the concept of confinement within QCD, which dictates that quarks and gluons cannot exist independently in nature and are therefore "forced" to confine within hadrons. According to this model, the colour confinement field, responsible for binding quarks and gluons, contracts into an extremely narrow flux tube between the coloured particles. Hence the name string, as this potential is very similar (if not equivalent) to a simple classical piece of string. In PYTHIA, strings are implemented at the end of the perturbative shower where the colour-chains produced during the shower are collected into colour singlets, called Lund strings. Each Lund string represents a confined gluonic flux tube [10]. As the quarks propagate outward from the production point in opposite directions, their energy and momentum are transferred to the Lund string, causing it to stretch. When sufficient energy is available, new quark-antiquark pairs can be generated in the string field, leading to its successive fragmentation, as depicted in Figure 3.

2.2.1 The Monash tune

The Monash 2013 tune [8][11], being the default tune in PYTHIA, was designed to focus on high-energy collisions without diffractive effects. The methodology of the Monash tune begins with initial assumptions about particle production, hadronization and high-energy physics. Parameters are adjusted by comparing model outputs with experimental data, primarily from experiments at LEP and SLAC, from electron-positron collisions. To prevent overfitting the data and to account for the breakup of protons certain parameter alterations were made.

Due to its reliance on the string breaking mechanism, the MONASH tune struggles to produce a sufficient number of baryons to match the yield that is measured experimentally. In order to overcome this issue, additional topologies were introduced.

2.2.2 Junctions tune

Junctions, [12][9] represent a different topology confinement in the PYTHIA event generator. Junction strings are a consequence of the SU(3) color structure inherent in QCD. This confinement binds together two or three fundamental particles (three being more common), known as partons, involved in the formation of hadrons, leading to final color-neutral configurations, giving rise to junctions, where the color strings intersect, as illustrated in Figure 4. Junctions, therefore, signify the convergence points of multiple color strings, illustrating the interactions between quarks and gluons. In PYTHIA simulations, the algorithms and models integrated within the event generator elaborate on the details of junction formation. These models take into account variables such as the color charges of participating quarks, the energy scale of the interaction, and the kinematic characteristics of the collision to depict the specific configuration of junctions.

Junction fragmentation occurs when the strings connecting the quarks are disrupted and transformed into final-state hadrons. Specifically, following the initial interaction, where color string between the patrons are created, hadronization ensues, resulting to the formation of color-neutral hadrons -mesons or baryons-. In the case of a three-quark system, the process of junction fragmentation involves the breaking of the color strings linking the quarks, which may lead to the generation of additional quark-antiquark pairs, which subsequently combine with the original quarks to form new hadrons. The outcome of junction fragmentation yields a spectrum of final-state hadrons, including those originating from the original quarks as well as any supplementary hadrons created during the fragmentation process. Although this would be how the broader process overview is modeled, in PYTHIA the precise implementation of junction fragmentation involves complex algorithms and models that simulate the interaction and fragmentation of color strings connecting the quarks. Monash on the other hand while it does not directly specify the details of fragmentation in PYTHIA, it impacts the process of hadronization by adjusting relevant parameters.

Therefore, in PYTHIA, junctions offer an advantage over the MONASH tune in terms of baryon production. While the MONASH tune relies on the string breaking mechanism, which has limitations in accurately replicating experimental baryon yields, junctions introduce a more complex topological structure that allows the simultaneous creation of multiple quark-antiquark pairs. The increased baryon production in junctions stems from their ability to form baryons from three independent quarks, rather than relying solely on the simpler string fragmentation process. In this way, junctions seem to capture better the dynamics of hadronization in high-energy collisions, improving the accuracy of the simulations.
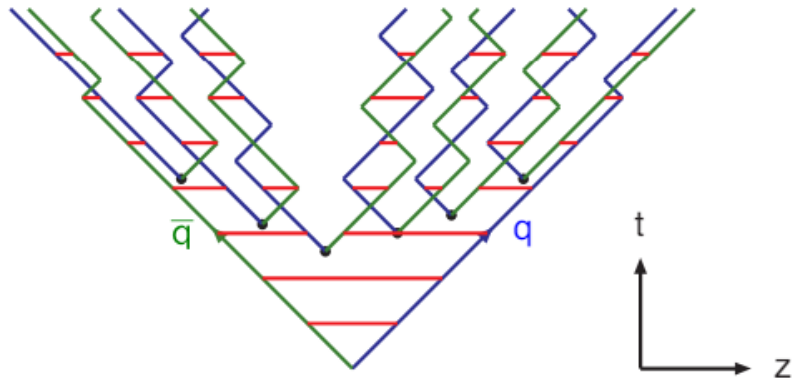
Figure 3: The hadronization process according to the Lund String Model. Figure taken from [13]
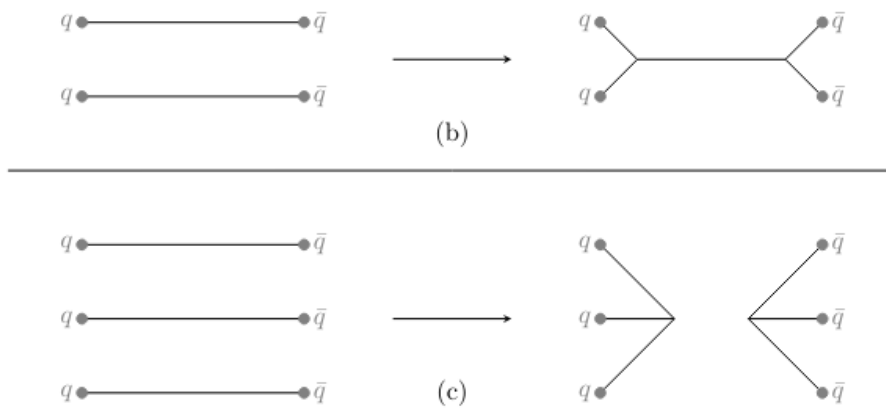

Figure 4: Junctions topology. Figure taken from [14]

3 Analysis procedures

3.1 Production details

It is essential to provide a concise overview of the **production details** prior to presenting the results. Specifically, in this study, simulations were conducted within the context of **proton-proton (pp) collisions**, generating a substantial dataset of **1.12 billion events** across both Monash and Junctions tunes. Noteworthy technical specifications include a **total center of mass energy of 14 TeV** and a **pseudorapidity coverage equal to 4**. The scope of this rapidity coverage aligns with that anticipated for the forthcoming heavy ion detector anticipated for installation post 2032. Additionally, the choice of **trigger - Ξ^- and Ω^-** - was deliberate, aimed at exploring their correlations with various associate particles across a wide transverse momentum (p_T) spectrum. This analysis, outlined in subsequent chapters, was performed using ROOT and focuses on the **Low-Low** (with a range starting from 1 to 3 GeV) and **High-High** (with its range being 8 and/or above GeV) **transverse momentum ranges**, details of which will be elucidated in the following sections.

3.2 Angular correlations/balancing

The analysis of particles' **azimuthal angular correlations** [15] has proven to be a valuable method used in particle physics, by giving insight into the mechanisms of particle production in high-energy collisions [16]. The difference between the azimuthal angle, $\Delta\phi$ from a pair of particles, which are hadronization products, is given by the formula $\Delta\phi=\phi_t$-ϕ_a, where ϕ_t is the trigger particle's azimuthal angle and ϕ_a is the associate particle's azimuthal angle. These are the main variables that consist the observable.

The correlation function that is measured is expressed in (1) . as the ratio of the signal over the background.

$$C = \frac{S(\Delta y, \Delta\phi)}{B(\Delta y, \Delta\phi)} \tag{1}$$

The signal S(Δy, $\Delta\phi$), as shown in (2) corresponds to particle pairs originating from the same event (collision), whereas the background B(Δy, $\Delta\phi$) (3), refers to the particle pairs coming from non-correlated events. More specifically, the numerator of the fraction comprises the study's physics along with effects related to the acceptance of the detector used. These effects are offset by the denominator, which exclusively considers non-physical correlations. These correlations are delineated by examining pairs from distinct events that, lack any physical correlation. This, however, is the generic interpretation, as in this study no detector was used, only simulations.

$$S(\Delta y, \ \Delta\phi) = \frac{1}{N(signal)} \frac{d^2 N signal}{d(\Delta y) d(\Delta\phi)} \tag{2}$$

$$B(\Delta y, \ \Delta\phi) = \frac{d^2 N back}{d(\Delta y) d(\Delta\phi)} \tag{3}$$

Each correlation function exhibits a distinct dependence on transverse momentum (p_T)

and/or multiplicity, reflecting its unique characteristics. In this study, azimuthal angular correlations serve as the primary tool for examining the behavior of selected charged hadrons in proton-proton (pp) collisions at a center-of-mass energy of $\sqrt{s} = 14$ TeV, simulated as was mentioned in the preceding subsection.

Additionally, particle balancing is an important aspect of the analysis. This involves ensuring that momentum, energy, and other conserved quantities are balanced before and after the collisions. Proper balancing helps verify the accuracy of the simulations and provides deeper insights into the collision dynamics and particle production mechanisms.

3.3 Example plots

In Figure 5 the trigger particle Ξ^- and the associate particle is Ξ^+. This represents the subtracted histogram, derived from the Opposite-sign (OS) minus the Same-sign (SS) histograms, both depicted in Figure 6a and Figure 6b respectively. The Opposite-sign histogram is essentially the signal, capturing our primary interest and it originates from particle pairs traced back at the same point in space and time, which are therefore correlated. The Same-sign histogram on the other hand represents the background, which we obtain from random pairs of particles -not originating from the same location- and thus are not correlated. This applies to all the plots that are presented in the following chapter. The subtracted plot reveals distinctive features on both the near and away sides, determined by the angle $\Delta\phi$, as illustrated in Figure 5.
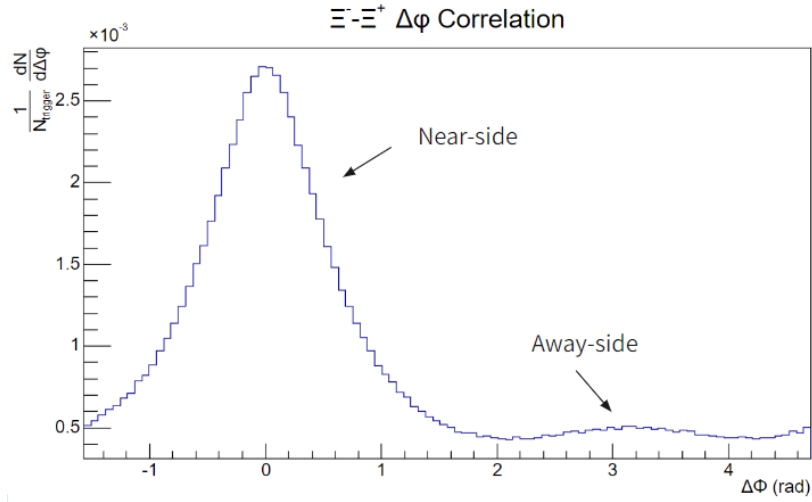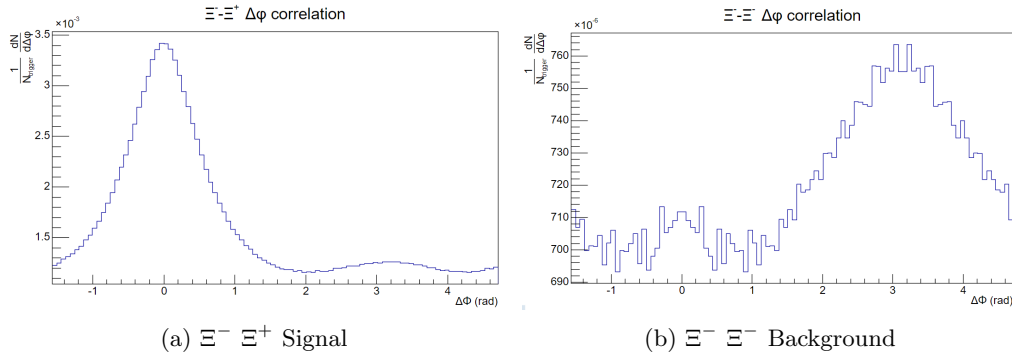

Figure 5: Ξ^- Ξ^+ Subtracted histogram

(a) Ξ^- Ξ^+ Signal

(b) Ξ^- Ξ^- Background

Figure 6: Ξ^- normalised per total trigger number azimuthal angular correlation plots in the Monash tune. The histogram in the left graph (a) refers to the signal and the histogram in the right graph (b) refers to the background.

4 Results

This section presents angular azimuthal correlation plots generated using two distinct P tunes (Tuning is when Pythia's settings are adjusted based on comparing PYTHIA 8.3's predictions with real data, in order for the simulations to be as closely as possible to the experimental data [8].). The study used two different trigger particles, Ξ^- (dss) and Ω^- (sss) in simulations conducted with both Monash and Junctions settings. Angular correlations were examined for various baryons and mesons in each scenario. It is important to note that all histograms presented below (for both Monash and Junctions) are normalised by the total trigger count.

4.1 Monash

In Figure 7 two Ξ^- azimuthal angular correlation plots are shown with the associate particles being charged Kaons (K), Λs and Ξs. The two plots, showing the subtracted distributions, refer to different p_T ranges. Figure 7a shows the case for low-low p_T, meaning that both the trigger and the associate particles have a p_T range from 1 to 3 GeV, while the Figure 7b on the right is the high-high p_T case, which following the same logic as before means the two particles' p_T range (trigger and associate) is from 8 and above GeV. A peak is noticed in the near side (on the left side of the plot). This indicates that the two particles - the trigger and the associate particle - are "traveling" in the same direction, almost in parallel. There is a small angle between the particles, which is approximately zero (0) rad and it is attributed to the way hadronization works in PYTHIA. Moreover, a small away side is also visible mostly for the Kaons and the reason why is connected to the particles that were formed at the beginning of the collision. There is a small bump for each one of the baryons as well, although due to the scale that is used in this plot it is not clearly visible. Observing this Monash plot we see how Ξ^- seems to be better balanced by mesons compared to the baryons and how the $(\overline{\Lambda})$ baryons are more "favoured" compared to the Ξ^+ baryons.

In Figure 8 we repeat the same process as previously, having however the Ω^- as our trigger particle and later on studying its azimuthal angular correlations with the Ξ^+ and the Ω^+ as our associate particles. We notice how Ω^- is better balanced by Ξ^+ rather than Ω^+. The Ω particle, consisting of three strange quarks, is a rather unstable and heavy baryon (with its mass being 1672.4 MeV), much heavier than the Ξ baryon (having a rest mass of 1321.71 MeV), which is most likely the reason why the balancing for this pair takes place as such.

(a) For low-low p_T range $\rightarrow$ p_T from 1 to 3 GeV

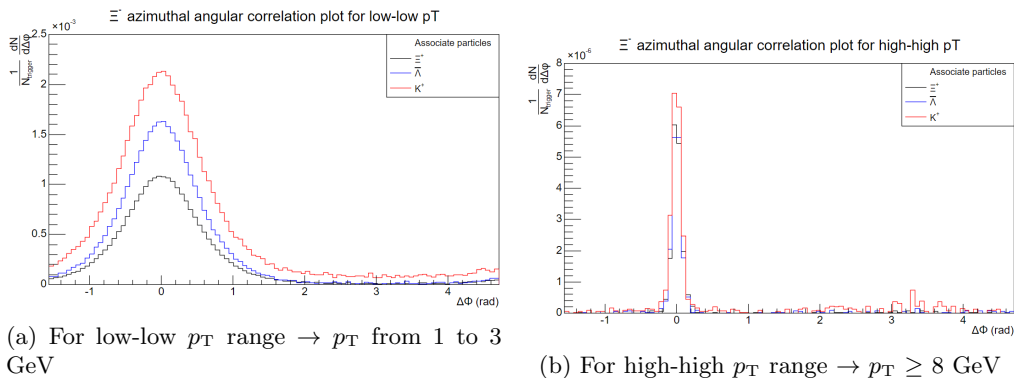(b) For high-high p_T range $\rightarrow$ $p_T \geq 8$ GeV

Figure 7: Ξ^- normalised per total trigger number azimuthal angular correlation (subtracted) plots in the Monash tune. The histograms in the left graph (a) are for low-low p_T bins, whereas the histograms in the right graph (b) are for high-high p_T bins.

The fact that the correlations are narrower in the high p_T case than in the low p_T one, as shown in Figure 7 and Figure 8, most likely comes from the fact that the two particles are part of the same "jet-like" structure and they are boosted with higher velocity, leading to tighter correlation than the low p_T case.
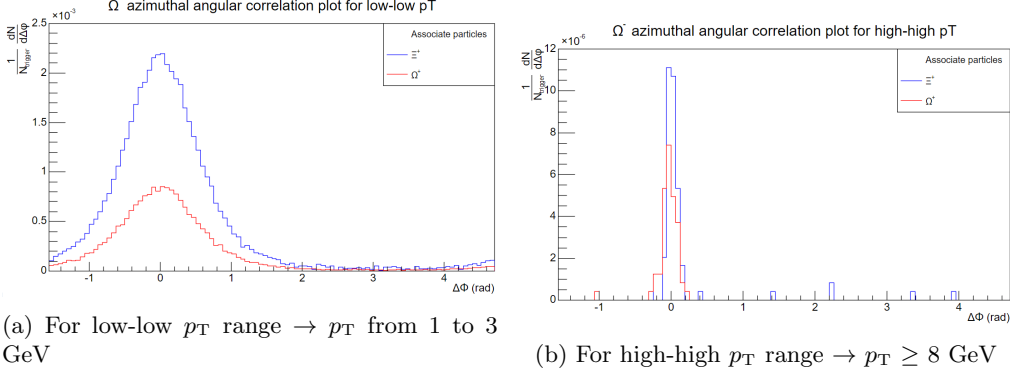

(a) For low-low p_T range → p_T from 1 to 3 GeV

(b) For high-high p_T range → $p_T \geq 8$ GeV

Figure 8: Ω^- normalised per total trigger number azimuthal correlation (subtracted) plots in the Monash tune. The histograms on the left graph (a) are for low-low p_T bins, whereas the histograms in the right graph (b) are for high-high p_T bins.

4.2 Junctions

Upon trying a different Pythia tune, Junctions, the previous results shown would be expected to be somehow altered. Repeating the same simulation steps as in Monash, the given results are demonstrated below.
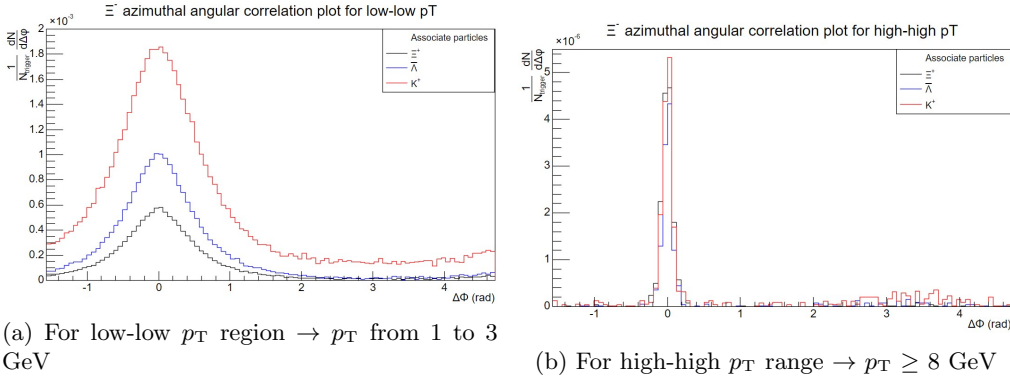

(a) For low-low p_T region → p_T from 1 to 3 GeV

(b) For high-high p_T range → $p_T \geq 8$ GeV

Figure 9: Ξ^- normalised per total trigger number azimuthal correlation plots in the Junctions tune. The subtracted histograms in the left graph (a) are for low-low p_T bins, whereas the subtracted histograms in the right graph (b) are for high-high p_T bins.

Figure 9a and Figure 9b as expected has a near side peak for each one of the associated particles. Ξ^- acts as the trigger particle and again our associates here are the following particles: $\Xi^+, (\overline{\Lambda})$ and K^+. Ξ^- seem to be balanced better with K^+, following by the $(\overline{\Lambda})$ baryons and lastly the Ξs. The low-low and high-high p_T cases have a similar structure in the Junctions, as the one they had in Monash. We notice that there are more statistics in the low-low p_T energetic range and less in high-high p_T one, most likely due to the production details that were chosen ($\sqrt{s} = 14 TeV$).
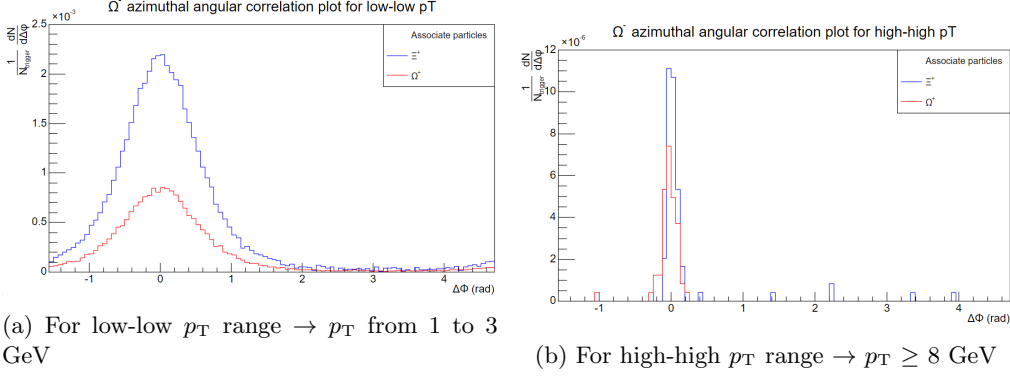
14

(a) For low-low p_{T} range $\rightarrow$ p_{T} from 1 to 3 GeV

(b) For high-high p_{T} range $\rightarrow$ $p_{\mathrm{T}} \geq 8$ GeV

Figure 10: Ω^- normalised per total trigger number azimuthal angular correlation plots in the Junctions tune. The subtracted histograms in the left graph (a) are for low-low p_{T} bins, whereas the subtracted histograms in the right graph (b) are for high-high p_{T} bins.

4.3 Comparison

Having presented all the results acquired from Monash and Junction tunes, in this subsection a comparison between the two different tunes' results will follow. Starting by comparing the results between Monash and Junctions for the Ξ^- baryon (Figure 7 and Figure 9), which are shown again as a comparison in Figure 11, we notice a significant increase in mesons and a smaller one, though still important in $(\overline{\Lambda})$ baryons in Junctions following by a decrease in Ξ^+ baryons. Considering how the Junctions' structure allows more the creation of baryons the increase in Ξ^+ and $(\overline{\Lambda})$ baryons was expected and taking into account how Junctions "favour" the balancing with the mesons, it was expected for the Ξ^--Ξ^+ pairs production to be somehow decreased.
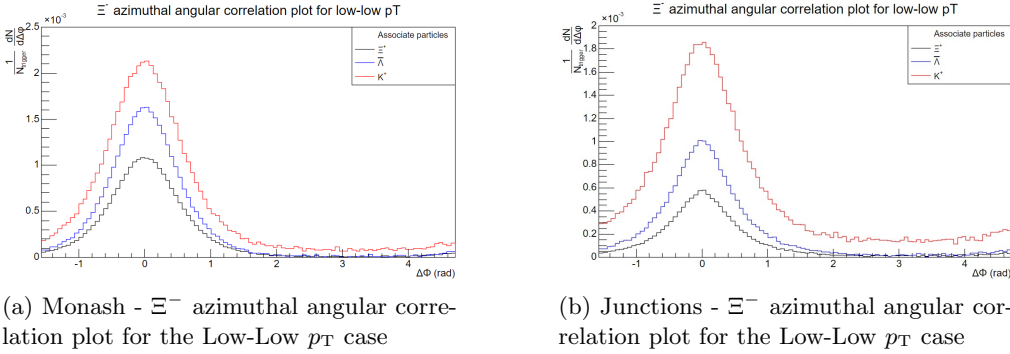

(a) Monash - Ξ^- azimuthal angular correlation plot for the Low-Low p_{T} case

(b) Junctions - Ξ^- azimuthal angular correlation plot for the Low-Low p_{T} case

Figure 11: Ξ^- azimuthal angular correlation plots for Monash (a) and for Junctions (b) for Low-Low p_{T} (from 1 to 3 GeV).

It is interesting to look at the Ω^- plots in Figure 12 as well and compare them. Through this comparison we notice an increase in both baryons, (Ξ^+ and Ω^+), in Junctions. It should be noted that the curves in Junctions appear decreased, but this is due to normalization (per total trigger number), which impacts the overall production values.

15

Therefore, we conclude that Junctions explain strangeness more adequately than Monash. Its energetic favourable structure allows more the creation of baryons and mesons, whereas Monash seems to fail to explain strangeness, especially the baryon production, as shown from the comparison we did.
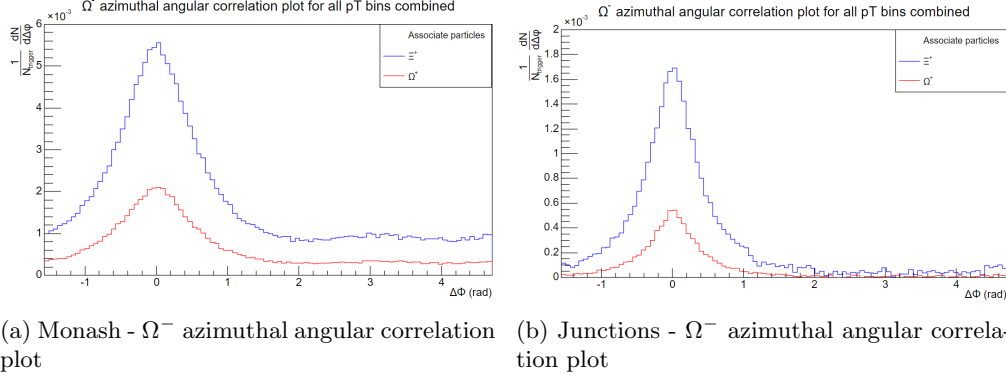

(a) Monash - Ω^- azimuthal angular correlation plot

(b) Junctions - Ω^- azimuthal angular correlation plot

Figure 12: Ω^- azimuthal angular correlation plots for Monash (a) and for Junctions (b) for Low-Low p_{T} (from 1 to 3 GeV).

5 Conclusion and outlook

In summary, this thesis presented a simulation study of strangeness, examining correlations among different strange hadrons across various transverse momentum (p_{T}) ranges in pp collisions at a center of mass energy $\sqrt{s}$=14 TeV.

This investigation focuses on the intricate dynamics of hadronization processes in high-energy pp collisions through comprehensive simulations using the PYTHIA event generator. By analyzing the azimuthal angular correlations of hadrons, particularly focusing on particles containing strange quarks, this study aims to enhance our understanding of the underlying mechanisms governing strangeness production.

The comparison between two distinct PYTHIA tunes, Monash and Junctions, has elucidated notable differences in their ability to explain strangeness production. While Monash provides valuable insights into the overall behavior of hadronization processes, it appears to fall short in adequately explaining strangeness production, particularly in baryon production. On the other hand, Junctions exhibit a more favorable structure that facilitates the creation of both baryons and mesons, resulting in a more accurate depiction of strangeness enhancement phenomena.

The observed correlations between trigger and associate particles in different transverse momentum ranges reveal intriguing patterns, suggesting that high-energy collisions lead to tighter correlations, possibly due to the increased velocity and jet-like structures of the particles involved.

Furthermore, the comparison between Ξ^- and Ω^- plots highlights the effectiveness of Junctions in explaining strangeness production more adequately than Monash. The increase in both baryons, Ξ^+ and Ω^+, in Junctions further supports this conclusion.

Overall, this research contributes to advancing our understanding of hadronization processes and strangeness enhancement phenomena in high-energy collisions. The findings underscore the importance of selecting appropriate simulation settings to accurately model complex particle interactions and phenomena. Future research in this field could focus on refining existing simulation models and exploring additional factors influencing strangeness production in high-energy collisions.

By connecting theoretical simulations with experimental observations, this study sets the stage for future developments in particle physics and provides valuable understanding into the basic properties of matter at the subatomic scale.

References

[1] Cush. File: Standard model of elementary particles. `https://en.wikipedia.org/wiki/File:Standard_Model_of_Elementary_Particles.svg`, 2024. Accessed: 2024-06-06.

[2] Mark Thomson. *Modern particle physics*. Cambridge University Press, New York, 2013.

[3] Aad et al. Observation of a new particle in the search for the standard model higgs boson with the atlas detector at the lhc. *Physics Letters B*, 716(1):1–29, September 2012.

[4] Chatrchyan et al. Observation of a new boson at a mass of 125 gev with the cms experiment at the lhc. *Physics Letters B*, 716(1):30–61, September 2012.

[5] Adams et al. Experimental and theoretical challenges in the search for the quark–gluon plasma: The star collaboration's critical assessment of the evidence from rhic collisions. *Nuclear Physics A*, 757(1–2):102–183, August 2005.

[6] Adcox et al. Formation of dense partonic matter in relativistic nucleus–nucleus collisions at rhic: Experimental evaluation by the phenix collaboration. *Nuclear Physics A*, 757(1–2):184–283, August 2005.

[7] J. Adam, D. Adamová, and Aggarwal et al. Enhanced production of multi-strange hadrons in high-multiplicity proton–proton collisions. *Nature Physics*, 13(6):535–539, April 2017.

[8] Christian Bierlich et al. A comprehensive guide to the physics and usage of pythia 8.3, 2022.

[9] Javira Altmann and Peter Skands. String junctions revisited, 2024.

[10] Cody B Duncan and Peter Skands. Fragmentation of two repelling lund strings. *SciPost Physics*, 8(5), May 2020.

[11] P. Skands, S. Carrazza, and J. Rojo. Tuning pythia 8.1: the monash 2013 tune. *The European Physical Journal C*, 74(8), August 2014.

[12] Jesper R. Christiansen and Peter Z. Skands. String formation beyond leading colour. *Journal of High Energy Physics*, 2015(8), August 2015.

[13] Roman Pasechnik and Michal Šumbera. Different faces of confinement. *Universe*, 7(9):330, September 2021.

[14] Leif Lönnblad and Harsh Shah. A spatially constrained qcd colour reconnection in pp, pa, and aa collisions in the pythia8/angantyr model. *The European Physical Journal C*, 83(7), July 2023.

[15] Daniela Ruggiano. Two-particle angular correlations of identified particles in pp collisions at $\sqrt{s} = 13$ tev with alice, 2024.

[16] ALICE Collaboration. The alice experiment – a journey through qcd, 2022.